Materials Advances

ROYAL SOCIETY OF CHEMISTRY

PERSPECTIVE

View Article Online
View Journal | View Issue

Cite this: *Mater. Adv.*, 2025, **6**, 7141

Beyond traditional photosensitizers in DSSCs: harnessing the optical properties of noble metal nanoclusters

Antonija Mravak,[a] Margarita Bužančić Milosavljević[b] and Martina Perić Bakulić*[a]

In an effort to reduce the carbon footprint, green alternative technologies such as dye sensitized solar cells (DSSCs) are being developed. In this evolving field, the search for efficient photosensitizers that can enhance light harvesting, charge transfer, and interfacial stability remains a central challenge. One promising direction for their development includes nanostructured materials, in particular, atomically precise noble metal bio-nanoclusters (bio–NCs). Because of their unique properties that can bridge the gap between classical bulk and quantum systems, they offer great potential as novel, non-traditional photosensitizers. In this Perspective, a computational chemistry-driven outlook is provided, developed in close collaboration with experimental insights, on recent advances in the study of noble metal bio–NCs. Emphasis is placed on their nonlinear optical (NLO) properties – an aspect crucial for DSSC performance, yet often overlooked. Three proposed photosensitizer systems are addressed: cyanidin–Ag_3 hybrid, Ag_3–DNA, and liganded Ag_{25}. Furthermore, heterometal atom doping has been discussed as a strategy to tune the electronic structure of NCs, thereby influencing their stability, catalytic properties, and photoluminescence. Additionally, as interactions with the semiconductor surface play an important role in charge separation, the anchoring modes of these systems on a TiO_2 model are proposed. By integrating insights from time-dependent density functional theory (TDDFT) with emerging experimental perspectives, this work aims to provide a deeper understanding of noble metal bio–NC properties towards revival in solar energy research.

Received 13th August 2025,
Accepted 15th September 2025

DOI: 10.1039/d5ma00901d

rsc.li/materials-advances

1. Introduction

Representing green and sustainable technology, dye sensitized solar cells (DSSCs) offer a promising alternative to conventional fossil fuel-powered devices. Starting with pioneering studies by Grätzel *et al.*,[1] a number of advantages have been demonstrated, from affordable and relatively easy production to integration into buildings,[2] with a maximum photoconversion efficiency of up to 15.2%.[3] Since then, DSSCs have evolved substantially with their first reported application-driven renaissance in 2012,[4] followed by different strategies for power conversion enhancement. As multi-component systems, DSSCs have been improved *via* targeting photosensitizers,[5–7] redox couples,[8–10] interface engineering,[11–13] light-trapping techniques,[14–16] or co-sensitization.[3,17,18]

More recently, growing global climate concerns have shifted the focus towards improving solar cell efficiency to address the sustainability of devices. Additional efforts have thus been made to develop greener solutions for each of the solar cell components. The period around 2020, accompanied by further increase in photoconversion efficiencies of DSSCs, is sometimes regarded as their second renaissance.[2]

At the core of the DSSC device lies the mesoporous semiconductor layer, typically TiO_2, with adsorbed dye molecules (photosensitizers). Upon illumination, the dye is excited and injects electrons into the TiO_2 conduction band. The oxidized dye is then regenerated by a redox mediator, which also transports charge through the electrolyte to the counter electrode *via* diffusion.[19] At the counter electrode, the redox mediator is reduced. Device operation is thus affected by several factors that govern the electron transport dynamics and contribute to the nonlinear behavior of DSSCs.[20] Some of these factors are light intensity, surface defects, trap-assisted recombination, charge accumulation at the semiconductor/electrolyte interface, and ion diffusion in the electrolyte. For instance, higher light intensities accelerate electron transport, while

[a] *Faculty of Chemistry and Technology, University of Split, Ruđera Boškovića 35, 21 000 Split, Croatia. E-mail: martinapb@ktf-split.hr*
[b] *Center of Excellence for Science and Technology-Integration of Mediterranean Region (STIM), Faculty of Science, University of Split, Ruđera Boškovića 33, 21000 Split, Croatia*

surface defects and trap states create localized energy levels that promote trap-assisted recombination.[19,21] In addition, charge accumulation at the semiconductor/electrolyte interface can lead to improved chemical capacitance and charge-transfer resistance.[22] Together, these processes strongly influence the stability and overall performance of DSSCs.

Since photosensitizers are responsible for electron injection into the semiconductor, they play one of the key roles in the solar cell cycle. For efficient device performance, photosensitizers must meet several key requirements.[19] Primarily, they should exhibit high thermal, electrochemical, and photostability, with the HOMO lying below the energy level of the redox mediator and the LUMO above the semiconductor band. The anchoring to the semiconductor must be strong, which is usually achieved through acidic anchoring groups. Furthermore, the absorption spectrum of the dye should extend from the visible to the near-infrared (NIR) region. These criteria ensure effective electron injection and dye regeneration.[19] In terms of sustainable photosensitizers, critical raw material-free (CRM-free) organic and natural dyes have been proposed as potential replacements for ruthenium-based systems.[2] However, due to limitations such as the use of harmful reagents in the synthesis of organic dyes, and the limited stability and efficiency of natural dyes, these systems still face challenges that have yet to be overcome.

Nanostructured materials, crossing the boundary between classical bulk and quantum-sized systems, offer potential for the development of novel, non-traditional photosensitizers with exceptional properties that satisfy the required preconditions.[23] Among them, atomically precise noble metal nanoclusters (NCs) based on Au, Ag, Pt, and Pd represent a new paradigm in solar and chemical energy conversion.[24] Neither a molecule nor a nanoparticle, but rather a molecule-like species, NCs possess discrete energy levels with strong fluorescence and a high surface-to-volume ratio. With dimensions below 2 nm, they show extraordinary properties arising from quantum size effects.[25] In this non-scalable regime, each atom can make a difference, since the removal, addition, or doping of one atom leads to new properties.

Generally, noble metal NCs are unstable under environmental conditions, necessitating specialized synthetic procedures for stabilization. When biomolecules are used for this purpose, the resulting structures are often termed bio–NCs[26] (see Fig. 1). They can be broadly categorized into two main types: liganded NCs and bio-nano hybrids. For structural functionalization, liganded NCs commonly utilize sulfur-containing ligands (cysteine (Cys), glutathione (SG), mercaptopropionic acid (MPA), bidentate dihydrolipoic acid (DHLA) and thiolated polyethylene glycol (PEG)). Bio-nano hybrids encompass all other unique structures of noble metal NCs synthesized with various possibilities for biomolecular protection (DNA scaffold, protein, *etc.*).[25,27–31] This protection significantly reduces the toxicity and aggregation of the NCs and enhances their biocompatibility. Furthermore, biomolecules can be functionalized for specific applications, such as improving their anchoring to semiconductors.

NCs are particularly intriguing because of their unique optical properties. Unlike larger plasmonic nanoparticles,

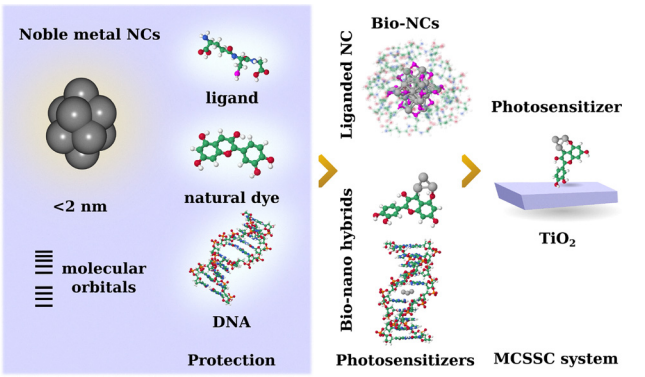

Fig. 1 Noble metal NC and biomolecular protection forming proposed photosensitizer systems in a metal cluster sensitized solar cell (MCSSC).

which are dominated by surface plasmon resonance (LSPR), the optical properties of noble metal NCs are, as discussed, molecule-like. The exact number of metal atoms is directly correlated with their electronic structure and thus with their absorption and emission spectra. This distinction makes them highly attractive for various optical applications. Many noble metal NCs show strong and tunable photoluminescence, often in the visible to NIR region, which are ideal characteristics for sensitizers in solar cells. Notably, the origin of their photoluminescence (PL) properties is not determined by only the metal core. The quantum yield of this luminescence can be influenced by the ligand shell, solvent, and structural integrity. For example, NCs with the same number of core atoms but different protecting ligands exhibit different PL properties.[32–36] In addition, bio–NCs exhibit strong nonlinear optical (NLO) responses conveniently tuned through cluster size, doping, and ligand exchange. Although this property is often overlooked in studies on solar cell performance, it is important to emphasize that enhanced two-photon absorption (TPA) and hyperpolarizability are related to improved light harvesting efficiency.[37,38]

Emerging new studies on theoretical and experimental characterization of NCs, along with their unique optoelectronic properties, have motivated us to provide a perspective on noble metal bio–NCs in DSSC applications. Going beyond previously reported metal cluster sensitized solar cells (MCSSCs), we aim to highlight the importance of NLO properties and introduce a new concept of bio-nano hybrid photosensitizers. In this context, we present systems based on noble metal NCs and natural dyes, as well as NC-DNA assemblies as potential sensitizers. While the focus of this Perspective is on a computational chemistry viewpoint, the discussion is framed within a theory–experiment dialogue to encourage collaborative efforts toward advancing noble metal bio–NC photosensitizers in DSSCs.

2. Liganded noble metal NCs for light harvesting

The slow progress in the research of liganded noble metal NCs as light harvesters has been attributed to the treatment of NCs

as traditional sensitizers despite their key differences.[23] Although power conversion efficiencies (PCEs) of liganded NCs are still far behind those of photosensitizers in DSSCs, the optimization of MCSSC systems has led to gradual improvements. A review of the work in this area over the past 15 years shows that most experimental efforts have focused on thiolated gold clusters.[39–49] Specifically, the first reported liganded metal clusters for light harvesting application were glutathione protected Au_n (n = 15, 18, 22, 25, 29, 33, and 39) with Au_{25} showing the best performance.[39]

An important step forward in developing MCSSCs was taken with the work of Kamat *et al.* who achieved a PCE of above 2% using an Au(0) core@Au(I)-thiolate shell structure and a Co^{2+}/Co^{3+} redox couple.[41] This was followed by a new record PCE of 3.8% in $Au_{18}SG_{14}$ operated using the I^-/I_3^- redox couple.[43] Similarly, a study on $Au_{11}SG_{11}$, $Au_{15}SG_{13}$, $Au_{18}SG_{14}$, $Au_{25}SG_{18}$ also identified $Au_{18}SG_{14}$ as the most efficient photosensitizer.[44] In general, the photovoltaic properties of liganded NCs have been demonstrated to be size dependent, influenced by their light absorption and excited state behavior.[44] Although earlier studies focused mainly on the photoelectrochemical response of glutathione liganded gold NCs, they were soon extended to systems with ligand protection based on BSA (bovine serum albumin), SBB (4-(*t*-butyl) benzylmercaptan), and MBA (4-mercaptobenzoic acid).[45]

An interesting way of applying gold NCs in light harvesting was the cosensitization of thiolated Au_x NCs with squaraine dye.[41] This approach revealed a broadened photoresponse, as Au NCs absorb below 500 nm and the dye in the 550–800 nm region. NCs had two functions: suppressing the photovoltage penalty and acting as a voltage booster and sensitizer. Interestingly, small structural changes within the NC core (for example in Au_{23}) were found to dramatically alter interfacial behavior and, as a result, overall photoconversion efficiency.[48]

Tatsuma *et al.* also proposed liganded silver,[50] palladium,[51] and platinum[51] clusters as potential photosensitizers. Compared to Au NCs, thiolated Ag NCs have been less studied and face two main limitations in solar energy applications: low stability and shorter excited state lifetimes.[52] While smaller Ag NCs have longer excited state lifetimes, higher stability, and lower self-recombination, their wider HOMO–LUMO gaps limit light absorption. Larger Ag NCs, on the other hand, absorb more widely but suffer from poor stability and fast recombination.[53] This presents a challenge when selecting the most suitable Ag NC size for the light harvesting application. In this regard, among a series of glutathione capped Ag_n (n = 15, 25, and 29) systems, Ag_{15} showed the highest internal quantum efficiency.[50] Other promising candidates included $Ag_{16}SG_9$[54] and $Ag_{25}SR_{18}$ (SR = 2, 4-dimethybenzenethiol).[55] In particular, it has been shown that liganded Ag_{25} is a stable photosensitizer that can boost photocatalytic efficiency.[55] When coupled with a CdS nanowire, it exhibits pronounced photoactivity and efficient charge transfer at the NC/CdS interface due to the favorable energy level alignment. This demonstrates the potential of Ag_{25} in solar energy conversion.

An effective approach for enhancing the PCE of liganded NCs is heteroatom doping. However, in the context of noble metal NCs, this strategy is more accurately described as heterometal atom doping. It enables a precise tuning of their electronic structure, which can, in turn, affect their stability, catalytic activity, and photoluminescence properties. These effects will be illustrated through selected examples presented later in this work. So far, the highest measured PCE among NC light harvesters is found for $AgAu_{17}SG_{14}$ NC with a PCE of 4.22%.[56]

2.1. Nonlinear optical properties of liganded noble metal NCs: hidden potential

In the context of Gratzel cells and the development of novel photosensitizers, research studies were focused on enhancing photovoltaic performance by optimizing the kinetics of TiO_2 adsorption and studying linear optical properties (one-photon absorption (OPA), fluorescence lifetime, fluorescence quantum yields, and PL measurements), all with the goal of achieving high absorption coefficients and broad spectral responses. However, one critical aspect often overlooked in sensitizer design was their NLO properties.

Nonlinear optics describes the complex, nonproportional relationship between an optical medium's induced polarization and the electric field of the incident light. This field becomes particularly relevant when materials interact with high-intensity light, such as from lasers, resulting in responses that go beyond simple linear interactions. The NLO properties have considerable potential to advance solar energy harvesting technologies. Although conventional solar cells predominantly rely on linear light absorption to convert photons into electrical energy, exploring the NLO properties may significantly improve both efficiency and functionality. A typical NLO active molecule consists of a π-conjugated system that incorporates electron-donating (D) and electron-accepting (A) groups, forming a donor–π–acceptor (D–π–A) architecture. This configuration is particularly well-suited to facilitating intramolecular charge transfer (ICT), a key mechanism underlying many NLO effects.

In the context of linear optics, the polarization induced in a material by an electromagnetic wave is directly proportional to the applied electric field. However, in nonlinear optics, this relationship becomes non-proportional at high field intensities, giving rise to a range of nonlinear responses that can be harnessed for advanced optoelectronic applications. In nonlinear optics the connection of polarization and electric field is complex and it can be expanded into Taylor power series:

$$\vec{P}_{NL} = \varepsilon_0[\chi^{(1)} + \chi^{(2)}\vec{E} + \chi^{(3)}\vec{E}\vec{E} + \ldots]\vec{E}, \quad (1)$$

where $\chi^{(1)}$ is the linear optical susceptibility and $\chi^{(2)}$ is the second-order nonlinear optical susceptibility. Furthermore, the $\chi^{(2)}$ term is responsible for second harmonic generation (SHG), where light at frequency ω is converted into light at 2ω (double the frequency, half the wavelength). This occurs for asymmetric systems. $\chi^{(3)}$ is the third-order nonlinear optical susceptibility that gives rise to effects such as third harmonic generation (THG) (converting ω to 3ω), TPA, and the optical Kerr effect (where the refractive index changes with light intensity). Materials can exhibit these effects regardless of their symmetry.[57–59]

TPA is a third-order nonlinear optical process in which two photons are simultaneously absorbed, promoting the system to an excited state with an energy equivalent to the sum of the two photon energies. To quantify the TPA of an individual molecule, the TPA cross-section, denoted as $\sigma_{TPA}(\omega)$, is commonly used. The quantity is typically expressed in units of 10^{-50} cm^4 s/photon, a unit also known as the Göppert-Mayer (GM) unit, named in honor of Maria Göppert-Mayer, who created the theoretical basis for investigations using the double-photon effect.[33,60] The TPA cross-section in SI units can be written as follows:

$$\sigma_{TPA}(\omega) = \frac{\alpha_2(\omega)\hbar\omega}{N} \quad (2)$$

where • $\sigma_{TPA}(\omega)$: two-photon absorption cross-section [cm^4 s/photon per molecule]
• $\alpha_2(\omega)$: two-photon absorption coefficient [cm W^{-1}]
• $\hbar$: reduced Planck constant [J s]
• ω: angular frequency of the photon [rad s^{-1}]
• N: number of molecules per unit volume [molecules per cm^3]

Noble metal NCs, particularly those of gold and silver, are exceptional materials in nonlinear optics. Their molecular-like behavior and distinct electronic transitions provide specific pathways for multiphoton absorption and other nonlinear interactions. In particular, in ligand-protected NCs, charge transfer processes between the metal core and the surrounding ligands can significantly enhance their nonlinear optical coefficients, mimicking the D–π–A molecular system.

2.2. "Ligand-core" NLO phores: a multishell perspective

Ligand-protected noble metal NCs can be conceptualized as a multishell system composed of three regions: the metallic core, the metal–ligand interface, and the ligand shell.[25] Each of these layers plays a crucial role in defining the structural and electronic properties of the noble metal NCs. The metal core typically consists of a compact cluster of noble metal atoms. Often forming well-defined staple motifs, the interface is characterized by strong metal–ligand interactions, particularly in thiolate-protected systems. The ligand shell further stabilizes the NCs and contributes to their solubility and surface chemistry. The ligands can act as electron donors or acceptors, facilitating charge transfers and increasing the overall hyperpolarizability. A representative example is $Ag_{25}(SG)_{18}$, often referred to as the "golden" silver nanoparticle due to its structural and electronic similarity to its familiar gold analogue, Au_{25} $(SR)_{18}$.[61] As shown in Fig. 2, the metallic core is a 13-atom icosahedral silver unit, surrounded by a network of Ag–S bonds at the metal–ligand interface, which form staple-like structures. These structural motifs are not passive. They enable charge transfer processes from the ligand shell to the metal core, which is essential for tuning the NC's optical and electronic properties. This class of ligand-protected noble metal NCs is also termed "ligand-core" NLO phores, emphasizing the cooperative interaction between the ligand shell and the metal core in generating nonlinear optical responses such as two-photon absorption. Recently, increasing attention has been

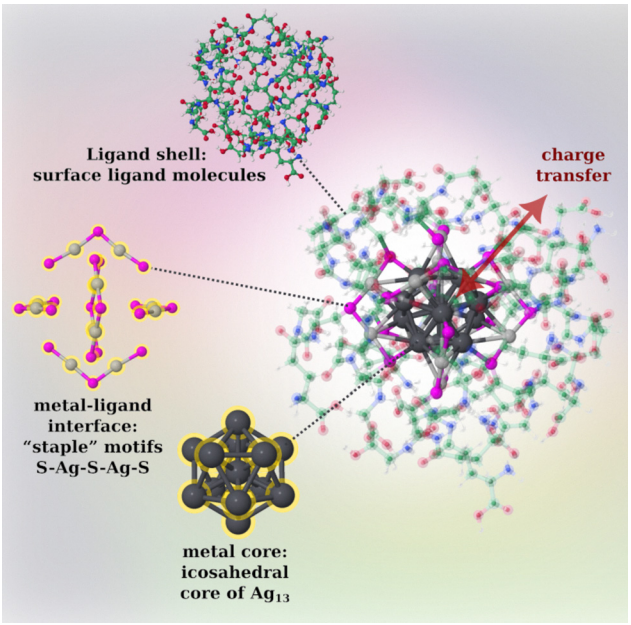

Fig. 2 Multishell perspective of glutathione liganded $Ag_{25}SG_{18}$: metal core, metal–ligand interface, and glutathione ligand shell.

directed toward investigating the TPA properties of ligand-protected noble metal NCs for applications in nano-biosensing and medical diagnostics. The nonlinear behavior enables deeper tissue penetration and higher spatial resolution in imaging applications.[62–65]

The TPA cross-section of bio–NCs is orders of magnitude greater than that of commercially available dyes. This significant enhancement in their NLO properties arises from a delicate interplay of resonance effects and large transition dipole moments. Furthermore, structural asymmetry inherent to the metal core itself or introduced by an uneven arrangement of surface ligands can dramatically enhance the second-harmonic generation process.[33,66–70]

2.2.1. Tailoring NLO properties through heterometal atom doping of $Ag_{25}SR_{18}$. The liganded NC synthesis has undergone remarkable evolution, from bulk material production to engineering of nanostructures with atomic precision. The precise heterometal atom doping of liganded NCs is a prime example of this evolution. This advanced technique enables strategic integration of other metal atoms, a single or even a few atoms, into liganded NCs while taking care of suitable stabilizing ligands. Such precision leads to finely tuned electronic, optical, or catalytic properties that are uniquely determined by the specific atomic arrangement. Heterometal atom doping can largely improve the physicochemical performances *versus* homometallic NCs. However, the doping modes are not universal since they depend on the metal of choice. Multiple doping modes are also a versatile strategy to tune optoelectronic properties since they offer simultaneous doping of the central metal core, kernel shell doping, and ligand–core interface rich in metal–sulfur bonds.[77]

Heterometal atom doping presents a cost-effective strategy for exploring and enhancing MCSSC's optoelectronic properties. To

illustrate the application of liganded noble metal NCs in MCSSC energy harvesting, the well-known silver NC $Ag_{25}(SR)_{18}$ was selected as a model system. This NC, with SR = S–PhMe$_2$, was first synthesized and structurally characterized by Bakr and co-workers in 2015.[61] In a subsequent study, platinum and palladium atoms were for the first time successfully introduced into the central site of the metal kernel of the thiolated Ag_{25} cluster *via* single-atom doping.[78] Since then, several research efforts have been focused on investigating the properties of heterometal atom doping in $Ag_{25}(SR)_{18}$, particularly using platinum and gold doping strategies.[66,79–82] Some of the recent studies focused on the doping strategies of Ag_{25} NCs have aimed to enhance their nonlinear optical properties – for instance, the effect of multiple gold doping on two-photon absorption,[66] as well as the influence of precise single-atom doping with Pt, Pd, or Au on hyperpolarizabilities.[83]

Building upon this foundation, a recent study explored the impact of single-atom metal doping on the photophysical and NLO properties of silver NCs.[83] Specifically, the $Ag_{25}(SR)_{18}$ NCs were doped with single atoms of Pt, Pd, and Au. The aim was to investigate how such precise heteroatom substitutions influence two-photon excited photoluminescence and second-order nonlinear optical scattering properties, particularly the first-order hyperpolarizability. The first hyperpolarizability is denoted as $\beta(2\omega)$, where 2ω refers to the second harmonic frequency.[58] Among the doped NCs, Pt and Pd-doped Ag_{25} exhibited the most significant enhancement in NLO properties. The absorption spectra showed a notable blue shift, directly attributed to doping of the metal core. One-photon and two-photon excited photoluminescence spectra both showed enhanced emission intensity, with platinum doping having the most pronounced effect. The measured first hyperpolarizability $\beta(2\omega)$ values for these systems were up to an order of magnitude higher than those reported for $Au_{25}(SR)_{18}$, reaching as high as 1001×10^{-30} esu for the Pt-doped system. These are the highest values ever observed for ligand-protected NCs to date. Time-dependent density functional theory (TDDFT) calculations of OPA spectra for all systems of Ag_{25} as well as its Au, Pd, and Pt-doped variants, showed trends consistent with experimental measurements. A similar trend was observed in the TDDFT calculated hyperpolarizabilities upon blue-shifted excitation wavelengths.

Here, as shown in Fig. 3, we demonstrate TDDFT OPA and TPA simulations of single Pt-doped $Ag_{25}SR_{18}$ NC.[83] The short SCH_3 ligands are used to qualitatively explore the TPA spectra following Pt doping. The OPA spectra are located between 700 nm and 300 nm and are in qualitative agreement with experimental findings. Since the S_1 state in OPA is located around 560 nm, the lowest two-photon transition occurs at approximately 1120 nm, with a very low TPA cross-section. High TPA cross-sections were observed around 750 nm and 700 nm. Key contributing factors to the enhanced TPA cross-sections were proposed:[65] resonance between TPA and OPA states, large transition dipole moments resulting from ligand-to-core or core-to-ligand charge transfer, and non-uniform electronic distribution within the metal core.

The enhanced linear and nonlinear optical properties of doped $Ag_{25}(SR)_{18}$ NCs provide a strong rationale for their application in DSSCs. The blue-shifted absorption observed upon doping, especially with Pt and Pd, extends the photoresponse of the NCs toward higher energy photons, improving the overlap with the solar spectrum and thereby enhancing light harvesting efficiency. This is important for efficient light harvesting in DSSCs. Moreover, the strong TPA and high first hyperpolarizability ($\beta(2\omega)$) values indicate that these NCs can contribute through NLO processes under NIR excitation. Although conventional DSSCs operate under one-photon conditions, materials with high nonlinear responses provide new opportunities for advanced DSSC architectures, such as upconversion-enhanced[84] or multi-photon driven designs, where NIR photons can be utilized.

In addition to heteroatom doping, other strategies can also be envisioned for enhancing NLO responses of nanoclusters. Surface ligand engineering, including ligand exchange and ligand–shell or protein–shell rigidifying, can tune electronic coupling and light–matter interactions. Electron donating group-based ligands result in enhancing the PL intensity which directly favours charge transfer through metal–ligand interface directly influencing nonlinear optical properties.[69,85–88] The chirality of surface ligands plays a pivotal role in governing the optical properties of nanoclusters, whether the ligands are inherently chiral or achiral but are arranged in a manner that

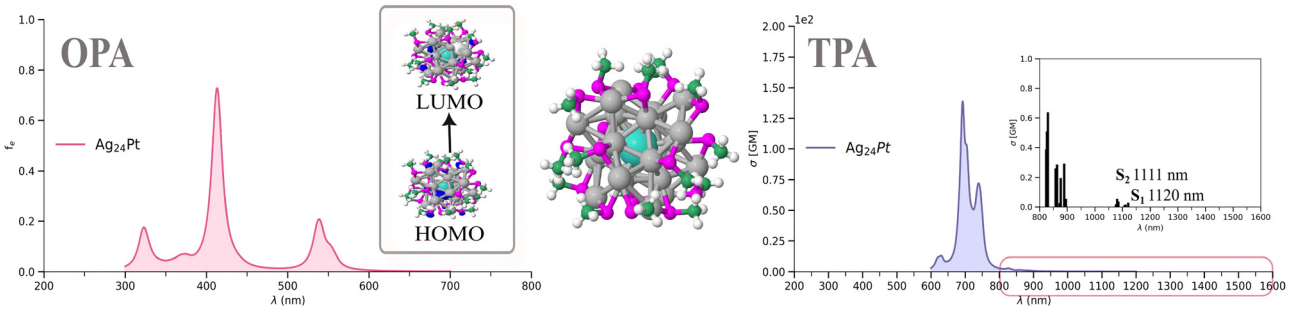

Fig. 3 TDDFT OPA (left) and TPA[71–73] (right) spectra calculated at the CAM-B3LYP[74]/def2-SVP[75] level of theory for $PtAg_{24}(SCH_3)_{18}$. For the Pt and Ag atoms the 19-electron relativistic effective core potential (19-e RECP) developed by the Stuttgart group[76] was implemented. DFT optimized structure with centrally doped single Pt atom is shown at the center, as well as HOMO–LUMO analysis. Atoms are colored by element: Ag in grey, Pt in turquoise, S in magenta, C in green, and H in white.

induces intrinsic chirality in the protected nanocluster.[89,90] Aggregation-induced fluorescence (AIF) represents another approach, where nanoclusters that are weakly emissive in solution become highly luminescent upon aggregation, and such enhanced excited-state responses could in principle be exploited to improve light–matter interactions and nonlinear optical processes.[91,92] Excited state dynamics offers another avenue, where tailoring relaxation pathways may optimize nonlinear absorption or scattering.[93] Finally, host matrix embedding and size effects, though more relevant for nanoparticles and plasmonic systems, highlight the diversity of approaches that have been explored in the wider NLO field.[94,95]

Taken together, the tunable electronic properties resulting from precise heteroatom doping, as well as by using other strategies, provide multiple routes to optimize electron injection efficiency and open-circuit voltage (V_{OC}) in DSSCs, while also pointing toward next-generation architectures capable of exploiting NLO effects.

3. Bio-nano hybrid systems for light harvesting

Previous studies on light harvesting have used the term bio-nano hybrids for natural pigments[96–101] including photoactive proteins[102–104] interacting with nanomaterials (quantum dots, nanotubes, and nanoparticles). In this Perspective, the concept of bio-nano hybrids refers specifically to systems based on atomically precise noble metal NCs and biomolecules. Their interaction leads to synergistic effects that are used for different purposes, such as label-free detection.[26] Consequently, they can serve as building units for optical, biosensing, and photocatalytic materials. For example, biosensing applications have been demonstrated in biomolecule-NC hybrid composed of a small Ag NC bound to a peptide. Enhanced optical absorption of this system arises from the coupling between electronic excitations within the NC and the π–π^* excitations of amino acids in the peptide.[27]

To explain the origin of absorption enhancement induced by metallic NCs, Bonačić-Koutecký *et al.*[27] compared the absorption spectra of pure peptides with those of cluster–peptide hybrids. In gas-phase experiments, charged Ag_3^+ and Ag_9^+ NCs were coupled with the dipeptide Trp-Gly and the tripeptide Trp-Ala_2. The resulting bio-nano hybrids showed stronger absorption and a shift into the ultraviolet region relative to pure peptides. The most intense peaks were attributed to the coupling of excitations within the NC with charge transfer excitations between the NC and the indole. In this context, NCs act as probes that enhance sensitivity of detection, and can serve as substitutes for conventional chromophoric dyes. Moreover, the absorption spectrum of neutral Cys-TrpAg_4 deposited on the MgO surface revealed a clear optical signature of the peptide. Essentially, NCs were shown to both immobilize the peptide and improve biosensing. Until recently, in addition to biosensing, these systems have been discussed mainly in the context of biochips and diagnostics. Here, we extend this concept to new bio-nano hybrid systems for solar cell applications, based on noble metal NCs and natural dyes.

3.1. Cyanidin–Ag_3

To address the limitations in stability and efficiency of natural-based DSSC sensitizers, we have introduced a new class of bio-nano hybrid sensitizers containing small silver clusters coupled with cyanidin dyes. In this section, we present our previous study on these hybrid systems[105] and extend it to our more recent work on their coinage metal-doped counterparts.[106] Compared to other works on natural-based sensitizers in DSSCs,[96–104] we have identified that the proposed bio-nano hybrids possess unique photovoltaic and optoelectronic properties that surpass those of pure natural dyes. Moreover, our study of the doping effect confirmed further improvements in their stability, photovoltaic parameters, as well as remarkable TPA. Notably, incorporating small noble metal NCs into cyanidin dye introduces donor–acceptor characteristics, inducing a favorable shift of the HOMO, LUMO levels that enables effective electron injection and dye regeneration. Enhancement in OPA and TPA originates from the coupling between the excited states of the dye and the NCs.

Specifically, in our previous work published in 2023,[105] we proposed hybrid systems based on Ag_n (n = 3, 5, 9, and 21, with 2, 4, 8, and 20 valence electrons, respectively) coupled to anthocyanidins. The latter were selected because they are readily available, nontoxic, and have already been investigated as photosensitizers.[109–112] However, their application in DSSCs has been limited as a result of poor stability, low efficiency, and unfavorable HOMO, LUMO energy levels. Coupling with NCs properly shifted their HOMOs and LUMOs and improved their optical properties. In addition, NCs introduced donor–acceptor regions important for charge separation. Subsequently, in our following work,[106] we explored the influence of coinage metal doping with Au and Cu atoms on the photophysical properties of these bio-nano hybrids.

Fig. 4 shows TDDFT calculated OPA and TPA spectra for the bio-nano hybrid cyanidin–Ag_3, as well as coinage metal doped cyanidin–Ag_2 Au and cyanidin–AgAuCu.[105,106] The OPA spectra for all three systems follow a similar trend, with two distinct absorption regions (around 300 and 500 nm). Among all systems, cyanidin–Ag_2 Au shows the strongest transition around 460 nm. This is directly reflected in the calculated light harvesting efficiencies: cyanidin–Ag_2 Au > cyanidin–AgAuCu > cyanidin–Ag_3. The electron injection values were negative for all systems, indicating a spontaneous process and satisfying an additional requirement for effective photosensitizers. Molecular orbitals reveal that the HOMO is delocalized over the dye and part of the silver trimer, while the LUMO is mostly delocalized on the NC.

The TPA spectra, with insets of the NIR region, shown in Fig. 4, reveal significant differences between the systems. Although cyanidin–Ag_3 exhibits a large cross-section around 460 nm, single gold doping enhances it approximately four times. Remarkably, heterometal doping with both Au and Cu increases the cross-section from the 10^8 GM to the 10^{10} GM

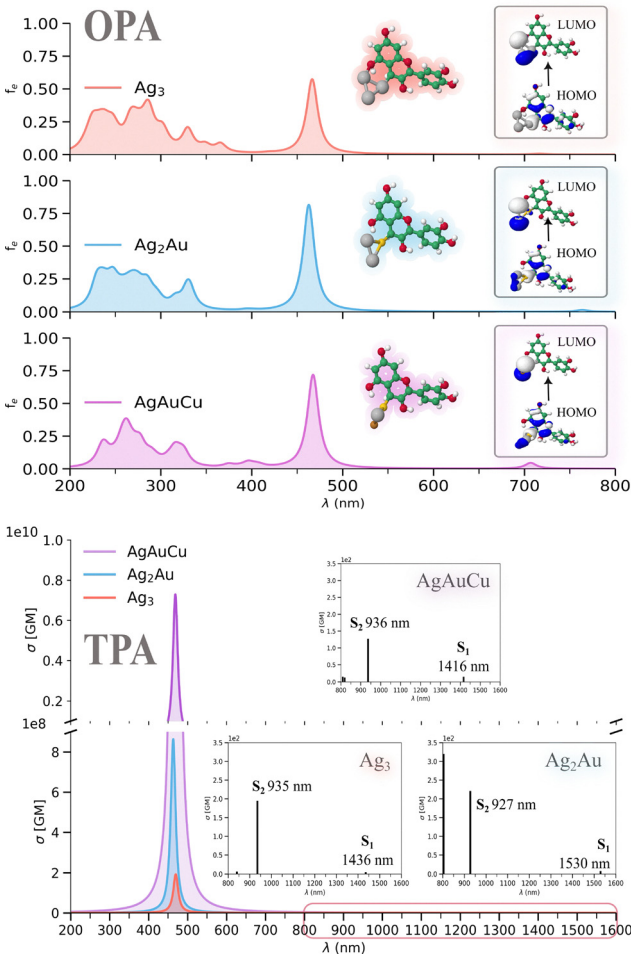

Fig. 4 TDDFT OPA (top) and TPA (bottom) spectra for cyanidin–Ag_3, cyanidin–Ag_2 Au, and cyanidin–AgAuCu calculated at the CAM-B3LYP[74]/def2-SVP[75] level of theory. For the Ag and Au atoms, the 19-electron relativistic effective core potential (19-e RECP) developed by the Stuttgart group[76] was implemented. Results are visualized based on our previous studies on monometallic[105] and doped[106] hybrids. The systems along with their HOMO, LUMO analysis are shown on the right. The insets in the bottom figure represent states in the NIR region. Atoms are colored by element: Ag in grey, Au in yellow, Cu in brown, C in green, O in red, and H in white.

range due to resonance between one-photon and two-photon excited states. These results confirm that doping increases the intensity of the cross-section, supporting the presence of charge transfer between the NC and the dye. The differences in TPA arise from variations in the electronic configurations of the coinage metal atoms and occupancies of the s and d orbitals.

To evaluate the properties of realistic DSSC systems, we also modeled cyanidin–Ag_3 and cyanidin–Ag_2 Au adsorbed on a TiO_2 semiconductor. In both cases, strong binding to TiO_2 was observed, with molecular orbitals indicating charge separation between the hybrid and the semiconductor surface. These findings, particularly their superior NLO and photovoltaic properties, suggest that bio-nano hybrids based on noble metal NCs and natural dyes have great potential for light harvesting applications.

3.2. Ag_3–DNA

DNA is a biopolymer with exceptional structural versatility. Beyond its role as the carrier of genetic information, DNA possesses several physicochemical properties that make it an attractive candidate for integration into optoelectronic devices. DNA has a well-ordered structure, rich chemical functionality, and programmable base-pairing interactions. It exhibits quasi-one-dimensional electronic conduction, facilitated by π–π stacking interactions between its base pairs, which can support coherent or hopping-based charge transfer over nanometric distances.[113] While DNA has been widely studied in nanotechnology, optoelectronics, and biosensing, its application in DSSCs remains largely unexplored, with only a handful of preliminary studies available in the literature.[114–116]

In our previous work published in 2018, we investigated the intriguing properties of silver trimers intercalated within DNA duplex structures, exploring the question: Why do silver trimers intercalated in DNA exhibit unique nonlinear properties that are promising for applications?[108] This theoretical study, based on experimentally and theoretically determined crystal structures of synthesized Ag–DNA complexes,[117] revealed that DNA not only stabilizes silver NCs but also modulates their electronic states through nucleotide base-specific coordination and conformational interactions. The Ag_3–DNA assemblies exhibited size- and environment-sensitive optical properties, with two-photon absorption cross-sections markedly enhanced in proximity to guanine- and cytosine-rich regions of the DNA duplex (see Fig. 5). These properties strongly suggest potential

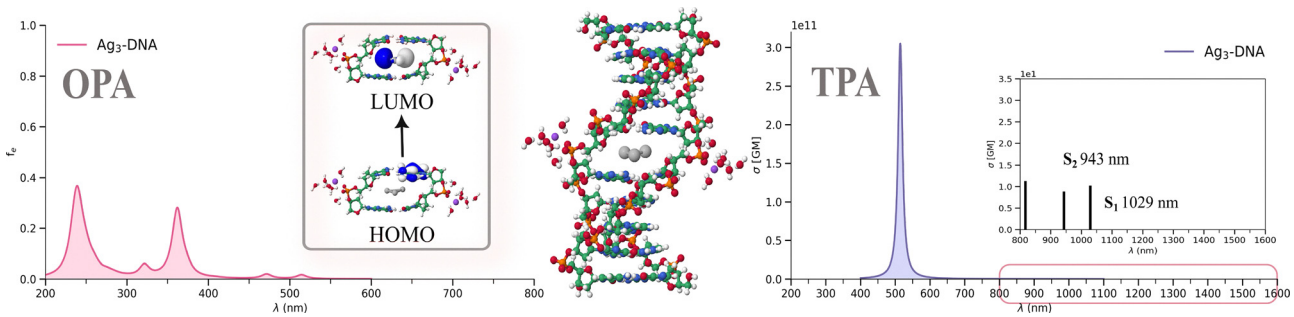

Fig. 5 TDDFT calculated OPA (left) and TPA (right) spectra at the PEQM level[107] for Ag_3^+ $(CGCGCGCGCG)_2$. The structure is shown in the central part. Results are visualized based on our previous study.[108]

utility in light-harvesting and electron-transfer applications. Since then, research on DNA-protected noble metal NCs has continued to expand.[118–124] Together, these findings laid the groundwork for viewing DNA not only as a biological scaffold, but as an active functional matrix for hosting and tuning noble metal NCs – an idea we now extend to the design of advanced DSSCs.

4. Anchoring onto the TiO_2 semiconductor

Another aspect of noble metal bio–NCs to discuss is their interface with the semiconductor surface. Although these interactions have been studied before, their true nature is only partially understood.[125] As demonstrated by several groups,[23,126–128] when bound to TiO_2, NCs behave as small bandgap semiconductors. This differs from traditional DSSCs and resembles quantum dot sensitized solar cells (QDSSCs).[125,129,130] However, they are considered a separate class of photosensitizers because they possess unique optoelectronic properties, show molecule-like behavior, and can transform into plasmonic nanoparticles upon irradiation.[23,125,131]

Efficient sensitization depends on the charge separation between the photosensitizer and the semiconductor. Therefore, it is important to examine adsorption modes, adsorption energies, and their influence on light harvesting. Generally, adsorption modes are determined by different interactions of the sensitizer anchoring groups with the surface of the semiconductor. These modes can be divided into strong covalent bonding, weaker electrostatic interactions, hydrogen bonding, hydrophobic interactions, van der Waals forces, and physical confinement within surface cavities.[19,132] Among them, chemisorption provides the strongest linkage through covalent bond formation, which enhances DSSC performance compared to weaker physisorption (*e.g.*, van der Waals forces).[19] Strong chemical binding also stabilizes the sensitizer and prevents its desorption from the surface.

Fig. 6(A–C) show the proposed binding modes of cyanidin–Ag_3, $Ag_{25}SG_{18}$, and Ag_3–DNA on the TiO_2 semiconductor model, considering the functional groups that are most likely to bind to TiO_2. The adsorption site for cyanidin–Ag_3 was determined based on the previous density functional theory (DFT) calculations[105] on a small TiO_2 fragment presented in Fig. 6D. Several binding orientations were examined, including binding through silver atoms, hydroxyl (–OH) groups, and combinations of the dye and the silver atoms. Anchoring over two hydroxyl groups *via* chemisorption was found to be the most energetically favorable. The formation of two Ti–O covalent bonds (d = 1.9 Å) results in adsorption energies around −2 eV confirming strong chemical bonding with the surface. The HOMO is mainly delocalized on the dye and partly on the NC, whereas LUMO is entirely delocalized on TiO_2, demonstrating clear charge separation between the sensitizer and the semiconductor.

Recently, as experimentally demonstrated for the glutathione protected Au cluster, anchoring to TiO_2 also proceeds over chemisorption.[49] This is possible since glutathione ligands

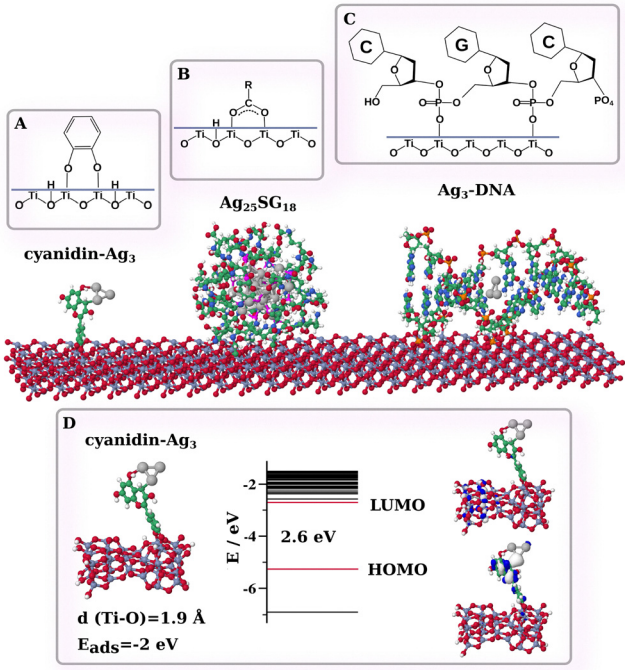

Fig. 6 Proposed anchoring modes of (A) cyanidin–Ag_3,[105] (B) $Ag_{25}SG_{18}$,[49] and (C) Ag_3–DNA[134] on the TiO_2 anatase model. (D) DFT optimized cyanidin–Ag_3@TiO_2 model at PBE[135]/def2-SVP[75] level of theory as reported in ref. 105 along with corresponding energy levels and the HOMO and LUMO. Atoms are colored by element: Ag in grey, C in green, O in red, S in magenta, P in orange, N in blue, Ti in lilac and H in white.

contain carboxylic (–COOH) groups that can form covalent bonds with the semiconductor surface. In general, –COOH can interact with TiO_2 over monodentate or bidentate modes. The bidentate mode can be chelating (both O atoms bind to a single Ti atom) or bridging (each O binds to a different Ti atom). Since the bidentate mode involves the formation of two Ti–O bonds, it ensures a stronger linkage compared to the monodentate mode.[133] The bidentate (bridging) mode was thus chosen to illustrate the binding of $Ag_{25}SG_{18}$ in Fig. 6B.

As for the Ag_3–DNA system, spectroscopic studies on DNA immobilization on TiO_2 have shown that the PO_4 phosphate backbone binds through chemisorption over strong P–O–Ti bonds[134] (*cf.* Fig. 6C). This chemical interaction enables increased electron mobility between DNA and the surface. Different DNA geometries can change the contact area between the photosensitizer and the surface, affecting both the adsorption strength and charge transfer. Additional theoretical and experimental studies on the interfaces between noble metal bio–NCs and the semiconductor could help elucidate their effect on solar cell performance and provide new strategies for its control.

5. Conclusions

Since the early 1990s, DSSCs have undergone significant evolution, marked by an initial revival nearly two decades later. Their most recent revival has been characterized by improved

efficiency and the development of strategies aimed at device sustainability. In this work, we present atomically precise noble metal bio–NCs as a promising new direction in the development of photosensitizers for light harvesting. Owing to their unique optoelectronic properties, they offer a novel paradigm in solar and chemical energy conversion. Over the past decade, slow but steady progress has been made in their application within MCSSCs, mostly concentrating on liganded noble metal NCs. We have extended that outlook to noble metal bio-nano hybrids, demonstrating their remarkable attributes. In particular, we have focused on the often overlooked NLO properties that could enable more efficient utilization of the solar spectrum and improved charge separation.

Bio-nano hybrids composed of natural dyes and small noble metal NCs are presented as a new class of sensitizers that show size- and composition-dependent NLO properties while meeting key requirements for DSSC application. In addition, the Ag_3–DNA system rich in guanine and cytosine has been demonstrated as potential light harvester that may also be suitable for inclusion in solar cells.

Generally, the two photon absorption cross-section of bio–NCs is several orders of magnitude higher than that of commercially available dyes. This enhancement arises from a synergistic interplay of resonance effects and large transition dipole moments. Furthermore, structural asymmetry, either intrinsic or introduced by uneven ligand arrangement, can significantly enhance second harmonic generation. Notably, in the non-scalable regime where each atom influences the overall properties of NCs, heterometal atom doping presents an effective strategy for fine-tuning the optoelectronic properties. Simultaneously, it can also shift the HOMO and LUMO energy levels in a favorable direction. These examples provide design principles and a framework for the rational development of next-generation photosensitizers with tunable optoelectronic properties.

Future progress in this field will depend not only on improved synthetic routes and strategies for tuning the optoelectronic properties of bio–NCs, but also on the development of more advanced theoretical approaches to model them. Since several processes occur at the bio–NC/semiconductor interface, more focus should be put on deciphering these phenomena. For instance, anchoring modes of the photosensitizers that affect electron transfer and, consequently, solar cell performance could be described in more detail by DFT/TDDFT. Another key challenge in the further development of bio–NC-based photosensitizers will also be ensuring their photochemical stability, both of the bio–NCs themselves and of the bio–NC/semiconductor assemblies. At the same time, more effort should be invested in the utilization of the known photocatalytic potential of NCs in the context of solar energy applications. Overall, when insights from theoretical methods are combined with developments of synthetic protocols, high-resolution spectroscopy, and systematic testing of solar cell prototypes, a theory–experiment synergy could provide valuable insights into the photoelectrochemical properties of these novel non-traditional photosensitizers.[125,136] Altogether, this perspective aims to encourage new theoretical and experimental findings on noble metal bio–NC photosensitizers, with a focus on their linear and nonlinear optical properties, in the hope of starting a new revival in solar energy research.

Author contributions

A. M.: conceptualization, methodology, investigation, writing – original draft. M. B. M.: data curation, formal analysis, visualization. M. P. B.: conceptualization, methodology, investigation, writing – original draft, supervision, funding acquisition, writing – review and editing.

Conflicts of interest

There are no conflicts to declare.

Data availability

All data supporting the findings of this study have been previously published and are available in the references cited in this article.

Acknowledgements

This research was supported by the project STIM-REI, Contract Number: KK.01.1.1.01.0003, funded by the European Union through the European Regional Development Fund – the Operational Programme Competitiveness and Cohesion 2014–2020 (KK.01.1.1.01). The authors acknowledge computational facilities of the University Computing Center in Zagreb and HPC within the STIM-REI project. The authors were supported by funding from ''Confined molecular systems: from a new generation of materials to the stars'' (COSY) – COST (European Cooperation in Science and Technology). The authors gratefully acknowledge Dr Vlasta Bonačić-Koutecký and Dr Rodolphe Antoine, whose pioneering experimental and theoretical research on noble metal NCs has greatly inspired their efforts to translate fundamental noble metal nanocluster knowledge into the development of dye sensitized solar cells.

References

1 B. O'Regan and M. Grätzel, *Nature*, 1991, **353**, 737–740.
2 N. Mariotti, M. Bonomo, L. Fagiolari, N. Barbero, C. Gerbaldi, F. Bella and C. Barolo, *Green Chem.*, 2020, **22**, 7168–7218.
3 Y. Ren, D. Zhang, J. Suo, Y. Cao, F. T. Eickemeyer, N. Vlachopoulos, S. M. Zakeeruddin, A. Hagfeldt and M. Grätzel, *Nature*, 2023, **613**, 60–65.
4 B. E. Hardin, H. J. Snaith and M. D. McGehee, *Nat. Photonics*, 2012, **6**, 162–169.
5 M. K. Nazeeruddin, F. De Angelis, S. Fantacci, A. Selloni, G. Viscardi, P. Liska, S. Ito, B. Takeru and M. Grätzel, *J. Am. Chem. Soc.*, 2005, **127**, 16835–16847.

6 A. Carella, F. Borbone and R. Centore, *Front. Chem.*, 2018, **6**, 481.
7 A. Colombo, C. Dragonetti, F. Fagnani and D. Roberto, *Electronics*, 2025, **14**, 1639.
8 S. M. Feldt, E. A. Gibson, E. Gabrielsson, L. Sun, G. Boschloo and A. Hagfeldt, *J. Am. Chem. Soc.*, 2010, **132**, 16714–16724.
9 A. Yella, H.-W. Lee, H. N. Tsao, C. Yi, A. K. Chandiran, M. K. Nazeeruddin, E. W.-G. Diau, C.-Y. Yeh, S. M. Zakeeruddin and M. Grätzel, *Science*, 2011, **334**, 629–634.
10 I. M. Abdellah, *RSC Adv.*, 2025, **15**, 9763–9786.
11 J. Krüger, R. Plass, L. Cevey, M. Piccirelli, M. Grätzel and U. Bach, *Appl. Phys. Lett.*, 2001, **79**, 2085–2087.
12 J. Xia and S. Yanagida, *Sol. Energy*, 2011, **85**, 3143–3159.
13 W. Ding, C. Bai, Y. Ren, D. Fang, J. Bai, J. Wen, B. Mi, D. Cao and Z. Gao, *Surf. Interfaces*, 2024, 104246.
14 I.-K. Ding, J. Zhu, W. Cai, S.-J. Moon, N. Cai, P. Wang, S. M. Zakeeruddin, M. Grätzel, M. L. Brongersma and Y. Cui, *et al.*, *Adv. Energy Mater.*, 2011, **1**, 52–57.
15 W.-Y. Rho, H.-Y. Yang, H.-S. Kim, B. S. Son, J. S. Suh and B.-H. Jun, *et al.*, *J. Solid State Chem.*, 2018, **258**, 271–282.
16 M. Manikandan, J. Anooja, K. Narayanan Unni and P. Sujatha Devi, *et al.*, *RSC Adv.*, 2025, **15**, 6171–6182.
17 M. J. Griffith, A. J. Mozer, G. Tsekouras, Y. Dong, P. Wagner, K. Wagner, G. G. Wallace, S. Mori and D. L. Officer, *Appl. Phys. Lett.*, 2011, **98**, 163502.
18 M. Onyemowo, Y. Unpaprom and R. Ramaraj, *Opt. Mater.*, 2024, **148**, 114860.
19 A. Hagfeldt, G. Boschloo, L. Sun, L. Kloo and H. Pettersson, *Chem. Rev.*, 2010, **110**, 6595–6663.
20 A. J. Frank, N. Kopidakis and J. Van De Lagemaat, *Coord. Chem. Rev.*, 2004, **248**, 1165–1179.
21 A. B. Muñoz-Garca, I. Benesperi, G. Boschloo, J. J. Concepcion, J. H. Delcamp, E. A. Gibson, G. J. Meyer, M. Pavone, H. Pettersson and A. Hagfeldt, *et al.*, *Chem. Soc. Rev.*, 2021, **50**, 12450–12550.
22 C. Zhang, Y. Huang, S. Chen, H. Tian, L. Mo, L. Hu, Z. Huo, F. Kong, Y. Ma and S. Dai, *J. Phys. Chem. C*, 2012, **116**, 19807–19813.
23 R. Khan, M. H. Naveen and J. H. Bang, *ACS Energy Lett.*, 2021, **6**, 2713–2725.
24 A. Munir, K. S. Joya, T. Ul Haq, N.-U.-A. Babar, S. Z. Hussain, A. Qurashi, N. Ullah and I. Hussain, *ChemSusChem*, 2019, **12**, 1517–1548.
25 R. Antoine and V. Bonačić-Koutecky, *Liganded silver and gold quantum clusters. Towards a new class of nonlinear optical nanomaterials*, Springer, 2017.
26 N. Goswami, K. Zheng and J. Xie, *Nanoscale*, 2014, **6**, 13328–13347.
27 V. Bonačić-Koutecky, A. Kulesza, L. Gell, R. Mitrić, R. Antoine, F. Bertorelle, R. Hamouda, D. Rayane, M. Broyer and T. Tabarin, *et al.*, *Phys. Chem. Chem. Phys.*, 2012, **14**, 9282–9290.
28 X.-R. Song, N. Goswami, H.-H. Yang and J. Xie, *Analyst*, 2016, **141**, 3126–3140.
29 I. Chakraborty and T. Pradeep, *Chem. Rev.*, 2017, **117**, 8208–8271.
30 G. F. Combes, A.-M. Vuković, M. Perić Bakulić, R. Antoine, V. Bonačić-Koutecky and K. Trajković, *Cancers*, 2021, **13**, 4206.
31 T. Pradeep, *Atomically Precise Metal Nanoclusters*, Elsevier, 2022.
32 R. Jin, C. Zeng, M. Zhou and Y. Chen, *Chem. Rev.*, 2016, **116**, 10346–10413.
33 V. Bonačić-Koutecky and R. Antoine, *Nanoscale*, 2019, **11**, 12436–12448.
34 T.-Q. Yang, B. Peng, B.-Q. Shan, Y.-X. Zong, J.-G. Jiang, P. Wu and K. Zhang, *Nanomaterials*, 2020, **10**, 261.
35 F. Muniz-Miranda, *Nanomaterials*, 2021, **11**, 2409.
36 Z. Liu, L. Luo and R. Jin, *Adv. Mater.*, 2024, **36**, 2309073.
37 D. S. Patil, K. C. Avhad and N. Sekar, *Comput. Theor. Chem.*, 2018, **1138**, 75–83.
38 F. Bardak and C. Bardak, *J. Mol. Struct.*, 2025, **1322**, 140528.
39 N. Sakai and T. Tatsuma, *Adv. Mater.*, 2010, **22**, 3185–3188.
40 A. Kogo, N. Sakai and T. Tatsuma, *Nanoscale*, 2012, **4**, 4217–4221.
41 Y.-S. Chen, H. Choi and P. V. Kamat, *J. Am. Chem. Soc.*, 2013, **135**, 8822–8825.
42 H. Choi, Y.-S. Chen, K. G. Stamplecoskie and P. V. Kamat, *J. Phys. Chem. Lett.*, 2015, **6**, 217–223.
43 M. A. Abbas, T.-Y. Kim, S. U. Lee, Y. S. Kang and J. H. Bang, *J. Am. Chem. Soc.*, 2016, **138**, 390–401.
44 K. G. Stamplecoskie and A. Swint, *J. Mater. Chem. A*, 2016, **4**, 2075–2081.
45 V. Jeseentharani, N. Pugazhenthiran, A. Mathew, I. Chakraborty, A. Baksi, J. Ghosh, M. Jash, G. Anjusree, T. Deepak and A. S. Nair, *et al.*, *ChemistrySelect*, 2017, **2**, 1454–1463.
46 M. A. Abbas and J. H. Bang, *ACS Energy Lett.*, 2020, **5**, 3718–3724.
47 L. L. Larina, O. Omelianovych, V.-D. Dao, K. Pyo, D. Lee and H.-S. Choi, *Nanoscale*, 2021, **13**, 175–184.
48 J. Lee, M. H. Naveen, J. Park, K. Pyo, H. Kim, D. Lee and J. H. Bang, *ACS Energy Lett.*, 2021, **6**, 2305–2312.
49 H. Naseer, M. Jeon, H. Kim and J. H. Bang, *Surf. Interfaces*, 2025, 106827.
50 N. Sakai, S. Nakamura and T. Tatsuma, *Dalton Trans.*, 2013, **42**, 16162–16165.
51 N. Sakai, T. Ikeda, T. Teranishi and T. Tatsuma, *ChemPhysChem*, 2011, **12**, 2415–2418.
52 M. A. Abbas, S. J. Yoon, H. Kim, J. Lee, P. V. Kamat and J. H. Bang, *ACS Appl. Mater. Interfaces*, 2019, **11**, 12492–12503.
53 B. A. Ashenfelter, A. Desireddy, S. H. Yau, T. Goodson III and T. P. Bigioni, *J. Phys. Chem. C*, 2015, **119**, 20728–20734.
54 M. S. Kim, M. A. Abbas and J. H. Bang, *Bull. Korean Chem. Soc.*, 2016, **37**, 791–792.
55 L. Zhan, J. Zhang, B. Ning, Y. He, G. Xiao, Z. Chen and F.-X. Xiao, *Inorg. Chem. Front.*, 2024, **11**, 7991–8002.
56 M. H. Naveen, R. Khan, M. A. Abbas, E. Cho, G. J. Lee, H. Kim, E. Sim and J. H. Bang, *Chem. Sci.*, 2020, **11**, 6248–6255.

57 J. L. Manthos, G. Papadopoulos and A. J. Sadlej, *Non-Linear Optical Properties of Matter*, Springer, 2010.
58 R. W. Boyd, *Nonlinear Optics*, Elsevier, 2020.
59 A. Dutt, A. Mohanty, A. L. Gaeta and M. Lipson, *Nat. Rev. Mater.*, 2024, **9**, 321–346.
60 M. Göppert-Mayer, *Ann. Phys.*, 1931, **401**, 273–294.
61 C. P. Joshi, M. S. Bootharaju, M. J. Alhilaly and O. M. Bakr, *J. Am. Chem. Soc.*, 2015, **137**, 11578–11581.
62 M. A. H. Muhammed and T. Pradeep, in *Luminescent Quantum Clusters of Gold as Bio-Labels*, ed A. P. Demchenko, Springer Berlin Heidelberg, Berlin, Heidelberg, 2010, pp. 333–353.
63 I. Díez and R. H. A. Ras, in *Few-Atom Silver Clusters as Fluorescent Reporters*, ed A. P. Demchenko, Springer Berlin Heidelberg, Berlin, Heidelberg, 2010, pp. 307–332.
64 S. H. Yau, O. Varnavski and T. I. Goodson, *Acc. Chem. Res.*, 2013, **46**, 1506–1516.
65 I. Russier-Antoine, F. Bertorelle, N. Calin, V. Sanader, M. Krstić, C. Comby-Zerbino, P. Dugourd, P.-F. Brevet, V. Bonačić-Koutecky and R. Antoine, *Nanoscale*, 2017, **9**, 1221–1228.
66 A. Pniakowska, K. Kumaranchira Ramankutty, P. Obstarczyk, M. Perić Bakulić, V. Sanader Maršić, V. Bonačić-Koutecky, T. Bürgi and J. Olesiak-Bańska, *Angew. Chem., Int. Ed.*, 2022, **61**, e202209645.
67 Y. Zeng, C. Comby-Zerbino, B. Grimm-Lebsanft, M. Teubner, S. Reichenberger, R. Antoine, M. Rübhausen, S. Barcikowski, W. J. Parak and I. Chakraborty, *ACS Appl. Nano Mater.*, 2025, **8**, 13611–13619.
68 W. Mohammad, K. D. Wegner, C. Comby-Zerbino, V. Trouillet, M. P. Ogayar, J.-L. Coll, R. Marin, D. J. Garcia, U. Resch-Genger, R. Antoine and X. Le Guével, *J. Mater. Chem. C*, 2023, **11**, 14714–14724.
69 M. Perić, Ž. Sanader Maršić, I. Russier-Antoine, H. Fakhouri, F. Bertorelle, P.-F. Brevet, X. le Guevel, R. Antoine and V. Bonačić-Koutecky, *Phys. Chem. Chem. Phys.*, 2019, **21**, 23916–23921.
70 A. Pniakowska, M. Samoć and J. Olesiak-Bańska, *Nanoscale*, 2023, **15**, 8597–8602.
71 L. Frediani, Z. Rinkevicius and H. Ågren, *J. Chem. Phys.*, 2005, **122**, 244104.
72 P. Norman, *Phys. Chem. Chem. Phys.*, 2011, **13**, 20519–20535.
73 P. N. Day, K. A. Nguyen and R. Pachter, *J. Chem. Theory Comput.*, 2010, **6**, 2809–2821.
74 T. Yanai, D. P. Tew and N. C. Handy, *Chem. Phys. Lett.*, 2004, **393**, 51–57.
75 F. Weigend and R. Ahlrichs, *Phys. Chem. Chem. Phys.*, 2005, **7**, 3297–3305.
76 D. Andrae, U. Häußermann, M. Dolg, H. Stoll and H. Preuß, *Theor. Chim. Acta*, 1990, **77**, 123–141.
77 X. Kang, Y. Li, M. Zhu and R. Jin, *Chem. Soc. Rev.*, 2020, **49**, 6443–6514.
78 J. Yan, H. Su, H. Yang, S. Malola, S. Lin, H. Häkkinen and N. Zheng, *J. Am. Chem. Soc.*, 2015, **137**, 11880–11883.
79 Y. Zhen, S. Jin, X. Kang, C. Xu, C. Fang, D. Hu and M. Zhu, *Inorg. Chem. Front.*, 2022, **9**, 3907–3914.
80 X. Lin, K. Sun, X. Fu, X. Ren, Y. Yang, C. Liu and J. Huang, *J. Phys. Chem. C*, 2021, **125**, 2194–2201.
81 M. S. Bootharaju, C. P. Joshi, M. R. Parida, O. F. Mohammed and O. M. Bakr, *Angew. Chem., Int. Ed.*, 2016, **55**, 922–926.
82 Y. Li, M. Zhou, S. Jin, L. Xiong, Q. Yuan, W. Du, Y. Pei, S. Wang and M. Zhu, *Chem. Commun.*, 2019, **55**, 6457–6460.
83 H. Yuan, I. Russier-Antoine, C. Moulin, P.-F. Brevet, Ž. S. Maršić, M. P. Bakulić, X. Kang, R. Antoine and M. Zhu, *Nanoscale Horiz.*, 2025, **10**, 314–321.
84 M. S. Eraky, S. S. Elsherif and M. M. S. Sanad, *J. Fluoresc.*, 2025, DOI: **10.1007/s10895-025-04198-x**.
85 Y. Zeng, S. Havenridge, M. Gharib, A. Baksi, K. D. M. Weerawardene, A. R. Ziefuß, C. Strelow, C. Rehbock, A. Mews and S. Barcikowski, *et al.*, *J. Am. Chem. Soc.*, 2021, **143**, 9405–9414.
86 F. Bertorelle, K. D. Wegner, M. Perić Bakulić, H. Fakhouri, C. Comby-Zerbino, A. Sagar, P. Bernadó, U. Resch-Genger, V. Bonačić-Koutecky and X. Le Guével, *et al.*, *Chem. – Eur. J.*, 2022, **28**, e202200570.
87 K. Sahoo and I. Chakraborty, *Nanoscale*, 2023, **15**, 3120–3129.
88 Z. Yang, Y. Wang, R. Zhang, T. Chen and J. Xie, *Adv. Mater.*, 2025, e08578.
89 S. Malola and H. Häkkinen, *Chem. Commun.*, 2019, **55**, 9460–9462.
90 Y. Zhu, J. Guo, X. Qiu, S. Zhao and Z. Tang, *Acc. Mater. Res.*, 2020, **2**, 21–35.
91 X. Kang, S. Wang and M. Zhu, *Chem. Sci.*, 2018, **9**, 3062–3068.
92 M. Zhu, Q. Yao, Z. Liu, J. Liu, M. Liu, M. Long and J. Xie, *J. Phys. Chem. Lett.*, 2022, **13**, 7722–7730.
93 S. Sharma, S. Das, K. Kaushik, A. Patra and C. K. Nandi, *Nanoscale*, 2025, **17**, 12858–12867.
94 G. Walters and I. P. Parkin, *J. Mater. Chem.*, 2009, **19**, 574–590.
95 Q. Yao, Z. Wu, Z. Liu, Y. Lin, X. Yuan and J. Xie, *Chem. Sci.*, 2021, **12**, 99–127.
96 C.-W. Chang, C.-H. Chang, H.-P. Lu, T.-K. Wu and E. W.-G. Diau, *J. Nanosci. Nanotechnol.*, 2009, **9**, 1688–1695.
97 R. Güzel, F. Yediyldz, Y. S. Ocak, F. Ylmaz, A. Ersöz and R. Say, *J. Photochem. Photobiol., A*, 2020, **401**, 112743.
98 S. N. Tamilselvan and S. Shanmugan, *Clean Energy*, 2024, **8**, 238–257.
99 U. Mahajan, K. Prajapat, M. Dhonde, K. Sahu and P. M. Shirage, *Nano-Struct. Nano-Objects*, 2024, **37**, 101111.
100 R. Chauhan, A. Srivastava, P. M. Shirage and K. Bala, *Sol. Energy*, 2024, **270**, 112369.
101 A. O. Soge, A. F. Oshin, C. Ulbricht, F. Mayr, O. D. Olukanni, O. F. Dairo, M. E. Sanyaolu, O. G. Adeyemi, S. Tekoglu and M. C. Scharber, *et al.*, *J. Electron. Mater.*, 2025, 1–15.
102 B. Mahyad, S. Janfaza and E. S. Hosseini, *Adv. Colloid Interface Sci.*, 2015, **225**, 194–202.
103 S. Janfaza, A. Molaeirad, R. Mohamadpour, M. Khayati and J. Mehrvand, *Bionanoscience*, 2014, **4**, 71–77.

104 M. Ghosh, *Nanomaterials-Based Composites for Energy Applications*, Apple Academic Press, 2019, pp. 161–184.
105 M. B. Milosavljević, A. Mravak, M. P. Bakulić and V. Bonačić-Koutecky, *RSC Adv.*, 2023, **13**, 6010–6016.
106 M. Bužančić Milosavljević, M. Perić Bakulić, Ž. Sanader Maršić, A. Mravak and V. Bonačić-Koutecky, *Nanomaterials*, 2024, **14**, 1034.
107 D. Hršak, J. M. H. Olsen and J. Kongsted, *J. Chem. Theory Comput.*, 2018, **14**, 1351–1360.
108 V. Bonačić-Koutecky, M. Perić and Ž. Sanader, *J. Phys. Chem. Lett.*, 2018, **9**, 2584–2589.
109 C.-Y. Chien and B.-D. Hsu, *Sol. Energy*, 2013, **98**, 203–211.
110 E. Marcano, *Energy Harvest. Syst.*, 2018, **5**, 29–38.
111 N. Y. Amogne, D. W. Ayele and Y. A. Tsigie, *Mater. Renewable Sustainable Energy*, 2020, **9**, 23.
112 N. Prabavathy, R. Balasundaraprabhu, S. K. Arne, G. Balaji, S. Prasanna, K. Sivakumaran, M. Kannan and R. E. Svein, *et al.*, *Optik*, 2021, **227**, 166053.
113 K. Ijiro and H. Mitomo, *Polym. J.*, 2017, **49**, 815–824.
114 K. Karthick, U. Nithiyanantham, S. R. Ede and S. Kundu, *ACS Sustainable Chem. Eng.*, 2016, **4**, 3174–3188.
115 Y. Wang, H. Yang and H. Xu, *Mater. Lett.*, 2010, **64**, 164–166.
116 J. Dagar, M. Scarselli, M. De Crescenzi and T. M. Brown, *ACS Energy Lett.*, 2016, **1**, 510–515.
117 D. Buceta, N. Busto, G. Barone, J. M. Leal, F. Domínguez, L. J. Giovanetti, F. G. Requejo, B. García and M. A. López-Quintela, *Angew. Chem., Int. Ed.*, 2015, **54**, 7612–7616.
118 Y. Chen, M. L. Phipps, J. H. Werner, S. Chakraborty and J. S. Martinez, *Acc. Chem. Res.*, 2018, **51**, 2756–2763.
119 D. J. E. Huard, A. Demissie, D. Kim, D. Lewis, R. M. Dickson, J. T. Petty and R. L. Lieberman, *J. Am. Chem. Soc.*, 2019, **141**, 11465–11470.
120 C. Cerretani, H. Kanazawa, T. Vosch and J. Kondo, *Angew. Chem., Int. Ed.*, 2019, **58**, 17153–17157.
121 A. González-Rosell and S. M. Copp, *Acc. Chem. Res.*, 2024, **57**, 2117–2129.
122 S. Malola and H. Häkkinen, *Chem. Commun.*, 2024, **60**, 3315–3318.
123 A. Rajeev and D. Bhatia, *Nanoscale*, 2024, **16**, 18715–18731.
124 R. R. Ramazanov, R. T. Nasibullin, D. Sundholm, T. Kurtén and R. R. Valiev, *J. Phys. Chem. Lett.*, 2024, **15**, 10710–10717.
125 M. A. Abbas, M. Jeon and J. H. Bang, *J. Phys. Chem. C*, 2022, **126**, 16928–16942.
126 I. Ji, M.-J. Park, J.-Y. Jung, M.-J. Choi, Y.-W. Lee, J.-H. Lee and J.-H. Bang, *Bull. Korean Chem. Soc.*, 2012, **33**, 2200–2206.
127 Y. Wang, X.-H. Liu, Q. Wang, M. Quick, S. A. Kovalenko, Q.-Y. Chen, N. Koch and N. Pinna, *Angew. Chem.*, 2020, **132**, 7822–7828.
128 R. Khan, M. H. Naveen, M. A. Abbas, J. Lee, H. Kim and J. H. Bang, *ACS Energy Lett.*, 2020, **6**, 24–32.
129 J. Zhang, C. Tang and J. H. Bang, *Electrochem. Commun.*, 2010, **12**, 1124–1128.
130 K. Tvrdy, P. A. Frantsuzov and P. V. Kamat, *Proc. Natl. Acad. Sci. U. S. A.*, 2011, **108**, 29–34.
131 S. Mai, J. Sun, Z. Fang, G.-B. Xiao and J. Cao, *Chem. – Eur. J.*, 2024, **30**, e202303973.
132 K. Kalyanasundaram and M. Grätzel, *Coord. Chem. Rev.*, 1998, **177**, 347–414.
133 M. K. Nazeeruddin, R. Humphry-Baker, P. Liska and M. Grätzel, *J. Phys. Chem. B*, 2003, **107**, 8981–8987.
134 M. Silva-Moraes, Y. Garcia-Basabe, R. de Souza, A. Mota, R. Passos, D. Galante, H. Fonseca Filho, Y. Romaguera-Barcelay, M. Rocco and W. Brito, *Spectrochim. Acta, Part A*, 2018, **199**, 349–355.
135 J. P. Perdew, K. Burke and M. Ernzerhof, *Phys. Rev. Lett.*, 1996, **77**, 3865.
136 T. Le Bahers, T. Pauporteé, P. P. Lainé, F. Labat, C. Adamo and I. Ciofini, *J. Phys. Chem. Lett.*, 2013, **4**, 1044–1050.